Coherent exciton-photon dynamics in semiconductor microcavities: The influence of inhomogeneous broadening

G. Bongiovanni and A. Mura
Istituto Nazionale di Fisica della Materia (INFM) and Dipartimento di Scienze Fisiche, Università degli Studi di Cagliari, via Ospedale 72, I-09124 Cagliari, Italy

F. Quochi, S. Gürtler, and J. L. Staehli
Institut de Physique Appliquée, Ecole Polytechnique Fédérale, PH-Ecublens, CH-1015 Lausanne, Switzerland

F. Tassone
Institut de Physique Théorique, Ecole Polytechnique Fédérale, PH-Ecublens, CH-1015 Lausanne, Switzerland

R. P. Stanley, U. Oesterle, and R. Houdré
Institut de Micro- et Optoélectronique, Ecole Polytechnique Fédérale, PH-Ecublens, CH-1015 Lausanne, Switzerland
(Received 16 July 1996)

We investigate a GaAs/(Ga,Al)As Fabry-Pérot microcavity, into which (In,Ga)As quantum wells have been inserted. The cavity is wedge shaped, i.e., the detuning between the bare-exciton resonance and the bare optical cavity mode depends on the spatial position on the sample. Linear transmission spectra reveal a well-resolved Rabi splitting of 8 meV at resonance, an inhomogeneously broadened exciton transition of 4–5-meV width, and an 0.7-meV-wide Fabry-Pérot mode. The time-resolved transmission exhibits deep beatings and a subpicosecond exponential decay: a behavior similar to that foreseen in the strong-coupling regime and in the absence of electronic disorder. Conversely, the four-wave mixing response appears weakly influenced by the cavity and not much different from what is expected for bare excitons. A photon echo, dephasing times as long as 50 ps, and only weak Rabi oscillations are observed. The experimentally observed features can be explained by a model based on the numerical solutions of the Maxwell-Bloch equations. This model confirms the dramatic influence structural disorder in the quantum wells has on the coherent nonlinear exciton-photon dynamics. [S0163-1829(97)00611-5]

INTRODUCTION

Semiconductor microcavities (MC's) are a very interesting physical system in which the confined electromagnetic modes interact with the exciton (X) states of the semiconductor.[1] MC's can be designed to be in the weak or in the strong coupling regime. In the latter case, the resonantly interacting X-photon modes, that are often referred to as cavity polaritons,[2] exhibit an anticrossing behavior with a vacuum Rabi splitting up to several meV.[1] If the X dephasing time and the photon lifetime are longer than the Rabi period, the coherent light-matter interaction manifests itself as an oscillation between X's and photons. In real structures, however, there always exists a certain degree of disorder, e.g., fluctuations of the well width or composition, which leads to the inhomogeneous broadening of the electronic levels. The spread of X energies is expected to induce an additional decay rate for the optical coherence that could heavily damp the X-photon oscillations in the strong-coupling regime.

The effects of the inhomogeneous broadening in MC's have been addressed very recently by various authors.[3–8] If the inhomogeneous width of the exciton levels is not larger than the Rabi splitting,[5] theoretical arguments indicate that close to resonance (1) the size of the vacuum Rabi splitting is weakly affected by disorder, (2) the split modes are homogeneously broadened, and (3) besides the polaritons there exists a continuum distribution of X states in the MC's that are optically active and whose energies are weakly affected by interaction with radiation.[6] The issues have very important implications, suffice it to say, on the effective temporal evolution of the linear and nonlinear coherent dynamics, and on the spontaneous and stimulated emission processes. The investigation on the subject is, however, still at the beginning. The large Rabi splittings observed in samples with a presumably important inhomogeneous broadening of the X line seem to confirm the limited influence of disorder on the splitting energy.[6,9] However, very little is known about the effects on the coherent temporal dynamics, which is of basic importance for the achievement of an effective strong coupling regime. To date, time-resolved (TR) reflectivity measurements with subpicosecond temporal resolution have been reported on samples in which the dynamics is mainly determined by the ultrashort photon lifetime of the bare cavity.[10] Four-wave mixing (FWM) has also been studied.[9] Deep quantum beats, a signature of the coherent energy exchange between X's and photons, also have been observed for large detunings between the X resonance and the cavity. The decay rates of the time integrated (TI) FWM signals could not, however, be explained in terms of a simple polariton picture, suggesting important disorder effects.

In this paper, we report on FWM experiments with quantum wells (QW's) embedded in a high-quality semiconductor MC. Transmission spectra reveal a Rabi splitting of 8 meV at resonance, and linewidths of 2 and 3 meV for the lower and upper polaritons, respectively. With respect to previous

measurements,[9] we have also resolved the nonlinear signal temporally. TR FWM is, in fact, the ideal spectroscopic tool to obtain conclusive information on the homogeneous and inhomogeneous broadening of the optically active states in the MC.[11] In addition, we also present TR transmission data. In comparison with reflectivity measurements, transmission permits a direct and accurate evaluation of the linear response[7] in both the time and spectral domains. The comparison of our experimental data with the solutions of the semiclassical Maxwell-Bloch equations allows us to clarify the way electronic disorder influences the coherent X-photon coupling in MC's.

EXPERIMENT

The specimen we investigated consists of six 75-Å-wide $In_{0.13}Ga_{0.87}As$ QW's at the antinodes of a $3\lambda/2$ long GaAs cavity. The two cavity mirrors are $AlAs/Ga_{0.9}Al_{0.1}As$ distributed Bragg reflectors consisting of 15 and 19.5 pairs having reflectivities of 98.5% and 99.8%, respectively. The detuning $\Delta \equiv h\nu_{\text{cavity}} - E_{\text{hh}X}$ between the Fabry-Pérot mode and the heavy-hole X mode varies across the sample because of the wedgelike shape of the cavity. Δ is estimated in a way similar to that explained in Ref. 12. The linewidth of the main transmission peak at large negative detunings (i.e., of the lower polariton which has practically photonic character) is $\gamma_c < 0.7$ meV, confirming the high quality of the cavity. On the other hand the upper polariton, which is practically an X and barely visible at this detuning, seems to be several meV wide. Degenerate FWM experiments were performed in the forward two-beam configuration, using nearly transform-limited 100 – 150-fs-long pulses centered in between the two polariton energies. In this configuration, two pulsed laser beams, $\mathbf{E}_1$ and $\mathbf{E}_2$ with wave vectors $\mathbf{k}_1$ and $\mathbf{k}_2$, respectively, are focused on the sample at nearly normal incidence. The two pulses arrive on the MC at times $t=0$ ($\mathbf{E}_2$), and $t=-\Delta T$ ($\mathbf{E}_1$). In the TI FWM experiments, the diffracted beam $\mathbf{E}_3$, propagating along $2\mathbf{k}_2-\mathbf{k}_1$, was dispersed in a spectrometer. The spectrally resolved nonlinear signal was detected by a slow detector (a photomultiplier or a charge-coupled semiconductor device) as a function of the delay ΔT between the incoming beams. The temporal evolution of the diffracted and transmitted beams was obtained by up-converting the signal with a reference pulse in a 1-mm-thick $LiIO_3$ crystal. The up-converted emission was detected by a photomultiplier as a function of the delay time of the reference pulse. All the experiments were performed at a temperature of 2 K.

EXPERIMENTAL RESULTS

Figure 1 shows the transmission spectra for different detunings Δ. An anticrossing behavior featuring a Rabi splitting of 7.8 meV is clearly observed. At resonance, i.e., at $\Delta=0$, the widths (full widths at half maximum) of the lower and upper energy transmission peaks amount to 2.3 and 3 meV, respectively. Given that at $\Delta=0$ the spectral broadening of the polaritons is expected to be the average between that of the bare X resonance (homogeneous *plus* inhomogeneous contributions[6]) and that of the photon mode, we estimate an X linewidth of 4 – 5 meV. This is at least one order of magnitude larger than the homogeneous linewidth of X's,[11] but compares favorably with the typical inhomogeneous broadening γ_{inh} caused by interface or compositional disorder. A further analysis shows that the lower polaritons can be fitted by Lorentzians with a linewidth that decreases for increasing detunings $|\Delta|$. Upper polaritons exhibit long tails at the high-energy side, however, interaction with light-hole X's and continuum states complicates the line shape analysis considerably.

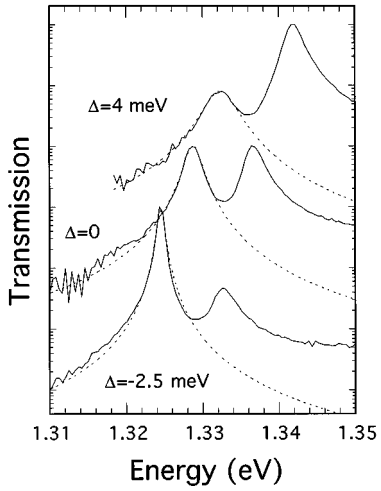

FIG. 1. Experimental transmission spectra, for different detunings Δ between the lowest cavity mode and lowest exciton state. The dashed lines are fits using a Lorentzian.

Figure 2 shows the TR transmission curves. In the range of excitation intensities we have used, i.e., for $I_{\text{ex}} \simeq 10^{10}$ photons/(pulse cm^2), the temporal behavior is independent of the laser intensity. In the limit of ultrashort pulse excitation, the evolution of the transmitted beam coincides with the linear response of the microcavity.[7] At large negative detunings, the long-time exponential decay approaches the response of the bare Fabry-Pérot resonator. From the decay rate $\tau \simeq$ 1 ps, we obtain a homogeneous broadening of 0.7

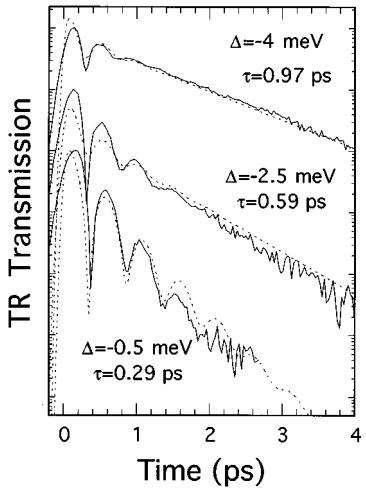

FIG. 2. Time-resolved (TR) transmission, measured (solid curves) at different detunings Δ between cavity and exciton. The dashed curves represent the numerical solutions of the Maxwell equations, as explained in the text. τ is the exponential decay time.

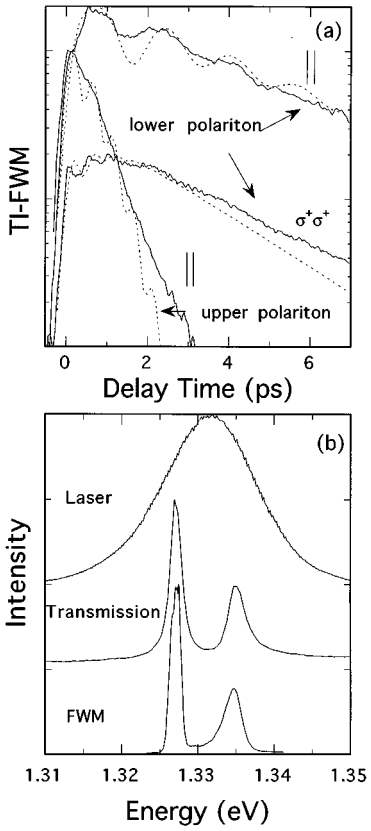

FIG. 3. (a) Experimental (solid) and theoretical (dashed) time integrated (TI) FWM signals, emitted at the lower and the upper polariton energies, vs delay time ΔT between the two laser pulses. The incident beams are colinearly ($\|$) or cocircularly polarized ($\sigma^+\sigma^+$). Detuning $\Delta=-2$ meV, and excitation intensity $I_{ex}\simeq 10^{11}$ photons/(pulse cm^2). (b) Spectra of the FWM emission for $\Delta T=0$ and colinearly polarized beams, of the incident laser pulses, and of the transmitted beams.

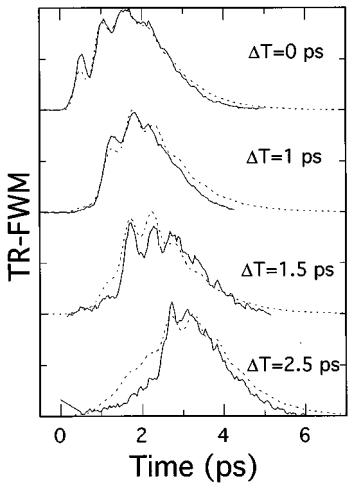

FIG. 4. Experimental (solid) and theoretical (dashed) time-resolved (TR) FWM signals for different delays ΔT in the $\|$ polarization geometry. Detuning $\Delta=-2$ meV, and $I_{ex}\simeq 3\times 10^{11}$ photons/(pulse cm^2). At $t=0$ the second pulse impinges on the sample.

meV, in excellent agreement with the cavity linewidth. The initial temporal dynamics exhibits oscillations, corresponding to an interference effect between the two polariton emissions. The oscillations disappear very quickly due to the shorter lifetime of the upper X-like mode (that can be estimated from its linewidth). Close to resonance, both the amplitude and decay time of the beats increase, as the oscillator strength and the lifetimes of the two polaritons become similar. Although the decay of the signal becomes much faster, it remains almost exponential with a long-time decay rate of 1/0.29 ps^{-1} (corresponding to a homogeneous broadening of 2.2 meV) that agrees very well with the spectral linewidth of the longer-living lower polariton. To estimate the inhomogeneous contribution, we have performed a least-square fit to the experimental data. Taking as fitting function the product of a Lorentzian and a Gaussian (which results from the Fourier transform of the convolution between the homogeneous and inhomogeneous spectral densities), the temporal width of the Gaussian results to be very long, confirming the *homogeneous* nature of the polariton broadening.[6]

Figure 3(a) shows the TI FWM signal versus delay time between the incoming beams for $\Delta=-2$ meV and $I_{ex}=10^{11}$ photons/(pulse cm^2). The difference between the dynamics of the linear (Fig. 2) and nonlinear responses is remarkable. The spectrum of the incoming laser pulses, the transmission spectrum, and that of the diffracted beam at $\Delta T=0$ are reported in Fig. 3(b). The peaks in the FWM response practically coincide with the energies of the two polaritons.[9] The temporal evolution of the nonlinear signal depends strongly on the emission energy. The decay time $\simeq 0.7$ ps at the upper polariton is very short. Conversely, the nonlinear signal at the energy of the lower polariton decays remarkably slowly with a time constant of 3.6 ps, for $I_{ex}\leqslant 3\times 10^{10}$ photons/(pulse cm^2) this lifetime becomes density independent and is as long as 13 ps (nearly 20 times longer than the τ measured in transmission). Very weak oscillations corresponding to the splitting measured in the transmission spectra are visible at short delays. Amplitude and period of these modulations are independent of excitation for $I_{ex}<10^{12}$ photons/(pulse cm^2). Beats with a longer period (1.8 ps) are also observed. The former oscillations are observable for all polarization configurations of the incoming beams, whereas the phase and amplitude of the latter are quite sensitive to the polarization geometry, and disappear completely for cocircularly polarized input beams. Most of these features, in particular the extremely long decay rates and their dependence on the emission energy, are distinctive of an inhomogeneously broadened X resonance. In addition, the slow beats and the dependence of the nonlinear signal on the polarization geometry are a clear signature of the excitation of bi$X$ states with antiparallel spins.[13]

In Fig. 4 the temporal evolution of the FWM signal for different time delays ΔT, for $\Delta\simeq -2$ meV and $I_{ex}\simeq 3\times 10^{11}$ photons/(pulse cm^2), has been plotted. The nonlinear emission shows beatings with a period corresponding to the Rabi splitting. Further, most of the signal is emitted at times $t\geqslant\Delta T$, featuring a photon-echo-like behavior. This time-delayed emission unambiguously proves that the levels giving rise to the nonlinear emission are *inhomogeneously* broadened. The nonlinear emission spectra feature peaks that are practically coincident with the polariton energies, because of the effect of spectral filtering of the MC on

the exciting electric fields and on the nonlinear emission. For the same reason the width of the echo, about 2 ps, is not equal to the inverse of the full inhomogeneous broadening $\gamma_{\rm inh} \simeq 4-5$ meV of the X distribution, which would yield a width of $\simeq 0.5$ ps.

THEORETICAL MODEL AND DISCUSSION

For the following discussion of the theoretical model, we assume that the interaction between exciton and radiation can be described in the framework of the Maxwell-Bloch equations,[14] in which the electromagnetic field is treated classically, and the exciton nonlinearities are accounted for in the density-matrix formalism. To obtain the linear and nonlinear responses, the Liouville equations for the density-matrix elements $\rho_{i,j}$ are solved in the rotating-wave approximation up to the third order in the incoming electric fields. $\rho_{i,j}$ are calculated for a five-level system, which accounts phenomenologically for one-exciton and two-exciton states.[13] The resulting equations read (neglecting the decrease of the intensity of the incoming laser fields $\tilde{\mathbf{E}}_1$ and $\tilde{\mathbf{E}}_2$, due to the generation of the weak nonlinear radiation[15])

$$\frac{\partial^2}{\partial z^2}\tilde{\mathbf{E}}_{1(2)}(\omega)+\frac{\epsilon\omega^2}{c^2}\tilde{\mathbf{E}}_{1(2)}(\omega)=0, \tag{1}$$

$$\frac{\partial^2}{\partial z^2}\tilde{\mathbf{E}}_3(\omega)+\frac{\epsilon\omega^2}{c^2}\tilde{\mathbf{E}}_3(\omega)=-\mu_0\omega^2\tilde{\mathbf{P}}_3^{(3)}(\omega), \tag{2}$$

$$\frac{\partial\rho_{i,j}(\omega_x)}{\partial t}=\frac{-i}{\hbar}[H(t),\rho(\omega_x)]_{i,j}-\frac{\rho_{i,j}(\omega_x)}{\tau_{i,j}}, \tag{3}$$

$$\mathbf{P}^{(1)[(3)]}(t)=\int g(\omega_x)\mathrm{Tr}[\rho^{(1)[(3)]}(\omega_x)\mathbf{d}]d\omega_x \equiv\int g(\omega_x)\mathbf{P}_x^{(1)[(3)]}(t)d\omega_x. \tag{4}$$

$\tilde{A}$ indicates the spectral component at the frequency ω of the quantity A. $\rho_{i,j}^{(n)}(\omega_x)$ represent the nth-order matrix density elements for excitons with frequency ω_x. $\mathbf{P}^{(1)}$ ($\mathbf{P}^{(3)}$) is the macroscopic linear (nonlinear) polarization. μ_0 and c are the permeability and light velocity in the vacuum, respectively. $g(\omega_x)$ is the spectral density of the inhomogeneous distribution of the X's. $H(t)$ is the usual semiclassical Hamiltonian of the five-level system interacting with the radiation field.[16] $1/\tau_{i,j}$ are the phenomenological decay rates of the density-matrix elements; in a two-level system featuring transitions between the crystal ground state, the lowest X state, one usually assumes $\tau_{1,2}=\tau_{2,1}\equiv T_X$ and $\tau_{1,1}=\tau_{2,2}\equiv T_l$ for the dephasing time and the longitudinal decay time of X's, respectively. $\mathbf{d}$ is the dipole moment operator. The QW is considered as a homogeneous medium with a local, macroscopic dielectric function,[6]

$$\epsilon(\omega)=\epsilon_b+\int g(\omega_x)\chi(\omega,\omega_x)d\omega_x, \tag{5}$$

with ϵ_b the background dielectric constant and $\chi(\omega,\omega_x)$ the local linear susceptibility of the X's with energy $\hbar\omega_x$.[17] $\epsilon=\epsilon_c=$const in the regions outside the wells. To simplify the calculations, we have considered a λ cavity containing only a single QW with an appropriate oscillator strength. Moreover, the distributed Bragg reflectors are replaced by two dielectric layers with a very high refractive index; this index has been chosen to reproduce the linewidth of 0.7 meV of the bare Fabry-Pérot mode as observed experimentally, and used throughout the calculations. The model is strongly simplified, but still contains the basic features of the X-photon coupling. First, Maxwell's equations (1) were solved for the spectral components $\tilde{\mathbf{E}}_1(\omega)$ and $\tilde{\mathbf{E}}_2(\omega)$ of the incident laser fields, by means of the standard transfer matrix method. The Fourier-transformed solutions $\mathbf{E}_{1(2)}(t)$ were then used to calculate the nonlinear polarization $\mathbf{P}_3^{(3)}(t)$ [Eqs. (3) and (4)]. Its spectral components $\tilde{\mathbf{P}}_3^{(3)}(\omega)$ were then introduced into the inhomogeneous wave equation (2) to obtain the propagating fields $\tilde{\mathbf{E}}_3(\omega)$ in the wells, the fields in the other regions of the cavity and outside were finally found by using again the transfer-matrix method.

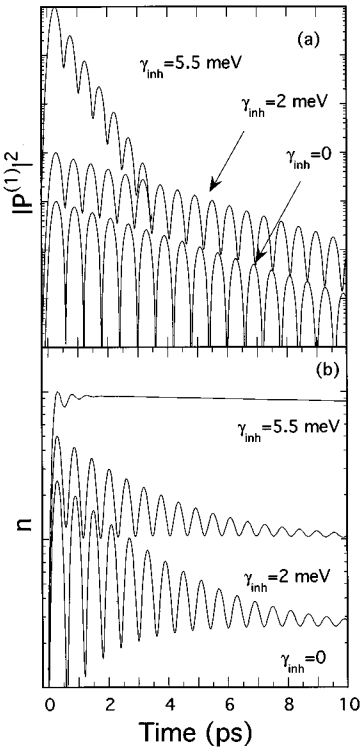

FIG. 5. (a) Square modulus of the linear polarization, $|P^{(1)}|^2$, and (b) exciton population n, vs time after excitation by a 100-fs-wide laser pulse, calculated at resonance ($\Delta=0$) and for different inhomogeneous X linewidths $\gamma_{\rm inh}$. Other parameters are given in the text.

We now discuss the effects of inhomogeneous broadening on the temporal evolution of the linear and nonlinear polarizations, as predicted by our numerical model. For simplicity, we refer to the numerical results obtained for a two-level system at resonance ($\Delta=0$), having a Rabi splitting of about 8 meV, an X dephasing time $T_X=20$ ps that is independent of energy, and a longitudinal decay time $T_l=100$ ps $\gg T_X$. Figure 5 shows the decay of $|P^{(1)}(t)|^2$ for different values of $\gamma_{\rm inh}$. As the linear polarization is induced by the electric field, but at the same time contributes to its buildup in the MC, $|P^{(1)}(t)|^2$ decays exponentially, featuring the

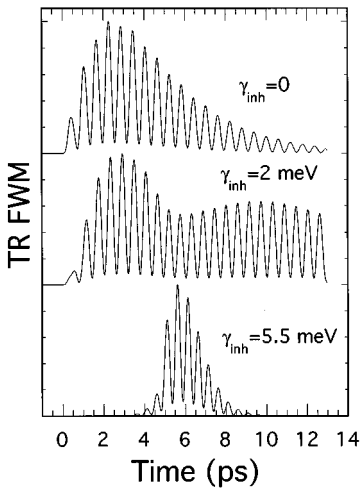

FIG. 6. Time-resolved (TR) FWM signals, calculated for different inhomogeneous X linewidths γ_{inh}, for $\Delta=0$ and $\Delta T=5$ ps. At $t=0$ the second pulse impinges on the sample. Other parameters are given in the text.

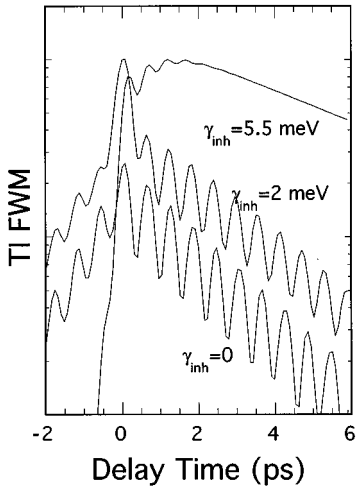

FIG. 7. Time-integrated (TI) FWM signals, emitted at the lower polariton energy, calculated for different inhomogeneous X linewidths γ_{inh}, and for zero detuning Δ. Other parameters are given in the text.

same time constant and beating period as the transmitted beam. In the homogeneous limit, the decay rate is $(\gamma_h+\gamma_c)/2$ (γ_h is the homogeneous X linewidth), while for strong inhomogeneous broadening (that, however, is smaller than the Rabi splitting) it becomes $\approx(\gamma_{\mathrm{inh}}+\gamma_c)/2$.[6] Concerning this, we point out that the Maxwell equations just require that $|P^{(1)}(t)|^2$ follows the decay of $|\mathbf{E}(t)^{(1)}|^2$. The component $|P_x^{(1)}(t)|^2$, representing the linear polarization of the X's with energy $\hbar\omega_x$, exhibits a very different and complicated behavior, which tends to the usual free induction decay with decay time $T_X/2$ in the limit of large inhomogeneous broadening. For $\gamma_{\mathrm{inh}}=0$ and $t\ll T_X$, $|P^{(1)}(t)|^2/N|\mathbf{d}|$ (N is the density of states of the two-level system) is equal to the whole X population $n(t)=\rho_{x,x}^{(2)}$ excited by the beam $\mathbf{E}_1(t)$.[18] Thus the oscillations of $|P^{(1)}(t)|^2$ also imply oscillations of $n(t)$, the very signature of the strong-coupling regime. At longer times, most of the X population $n(t)$ has become incoherent, hence at $t\gg T_X$ the decay time becomes equal to the longitudinal one T_l, and the Rabi oscillations disappear. In the case of strong inhomogeneous broadening (and $t\ll T_X$),

$$n(t)=\int g(\omega_x)n_x(t)d\omega_x=\frac{\int g(\omega_x)|P_x^{(1)}(t)|^2 d\omega_x}{N|\mathbf{d}|}$$
$$\neq\frac{|P^{(1)}(t)|^2}{N|\mathbf{d}|}, \tag{6}$$

where $n_x(t)$ is the population of X's with energy $\hbar\omega_x$. Thus, although $|P^{(1)}|^2$ decays rapidly and shows deep Rabi modulations, $n(t)$ experiences only weak Rabi oscillations and decays slowly with the longitudinal decay time T_l [see Fig. 5(b)]. Decreasing γ_{inh} to about 0.3 times the Rabi splitting, the behavior of $n(t)$ approaches that of the homogeneous case.

In analogy to what has been previously discussed for $P_x^{(1)}(t)$, the third-order polarization $P^{(3)}(t)$ is not expected to follow the polaritonlike behavior of $P^{(1)}(t)$. $P^{(3)}(t)$ is generated by the nonlinear interaction of the beams $\mathbf{E}_1$ and $\mathbf{E}_2$ with the QW's, but does not contribute to their buildup in the cavity (neglecting depletion). $P^{(3)}(t)$ excites the propagating cavity modes along the direction $\mathbf{k}_3$, the intensity of the outgoing diffracted beam is reported in Fig. 6, for different γ_{inh}, for $\Delta=0$ and for $\Delta T=5$ ps. For $\gamma_{\mathrm{inh}}=5.5$ meV, the FWM signal starts at $t\simeq\Delta T$, exhibiting a photon-echo-like behavior as a function of delay. The signal is modulated at the Rabi frequency. However, these oscillations do not correspond to an effective modulation of the X population $n(t)$, as shown in Fig. 5(b). For smaller values of the inhomogeneous broadening ($\gamma_{\mathrm{inh}}=2$ meV), a substantial fraction of the signal is also emitted at times $t<\Delta T$. For a further decrease of the inhomogeneous broadening, the echo disappears. However, the buildup of the FWM signal remains quite slow as it is determined by the cavity finesse and, hence, by the polariton lifetime.

For $\gamma_{\mathrm{inh}}=5.5$ meV, the emission is a photon echo, and thus the TI signal decreases with the delay time ΔT as $e^{-4\Delta T/T_X}$ (see Fig. 7), similarly to the case of bare quantum wells.[16] Decreasing γ_{inh}, the TI signal exhibits a behavior similar to that experienced by the population $n(t)$: the Rabi oscillations become more and more pronounced, and the decay rate increases [reaching $(\gamma_c+\gamma_h)/2$ in the limit $\gamma_{\mathrm{inh}}=0$]. Furthermore, the nonlinear signal is also emitted for negative delay times because of the increasing lifetime of the electric field in the cavity. Finally, we mention that the value of the longitudinal decay time T_l has a slight influence on the FWM signal, as the nonlinear process depends on the coherent fraction of the X population.

In the following, we compare the experimental results with the numerical solutions of the Maxwell equations, obtained for the above-mentioned five-level model. The calculated TR transmission decays are reported in Fig. 2; an inhomogeneous distribution of the X levels with a full width at half maximum of 5.5 meV has been taken. The oscillator strength has been adjusted to fit the frequency of the Rabi oscillations at resonance (the cavity finesse has been kept the same as above). The X dephasing times T_X have been assumed to vary across the transition, from 15 ps below the

resonance to 1.4 ps at and above the resonance.[19] This dispersion has been chosen to fit the different decay rates of the TI FWM signal emitted at the lower and upper polariton energies; it also corresponds to the well-known fact that the localized X states, which are in the low-energy tail of the inhomogeneously broadened X line, have much longer dephasing times than the extended states. Despite the simplicity of the model, the agreement with the experiment, in particular the dependence of the long-time exponential decay on the detuning, is remarkable. It is also worth pointing out that the strong variation of the X dephasing times with energy is essential to obtain the observed decay of the beat amplitude at $\Delta \approx 0$.

Figure 3 shows the comparison with the experimental TI FWM response. The dependence of the decay rate on the emission energies and the weak Rabi oscillations at the lower polariton are in good agreement with the experiment. The Rabi modulation of the TI traces of the upper polariton is, however, much weaker in the experiments. Possibly, this difference could be due to the presence of X continuum states which are ignored by the model. The beatings with the long period can be reproduced well by taking a bi$X$ binding energy of 2.5 meV.[20] Finally, the theoretically expected TR FWM response (dashed curves in Fig. 4) agrees quite well with the experimentally observed echolike behavior. The Rabi oscillations are much weaker than in Fig. 6, as much shorter X dephasing times at the lower-energy side of the resonance (2 ps) had to be taken. These shorter times have been chosen to fit the faster decay rates of the experimental TI signal caused by the higher excitation intensities used in the TR FWM experiments

CONCLUSION

In conclusion, the results presented here show the strong influence of the electronic inhomogeneous broadening on the coherent dynamics of the X-photon coupling in microcavities. In the sample we have investigated, featuring a Rabi splitting of 8 meV and a linewidth of the two polaritons of about 2.5 meV, the effect of the inhomogeneous distribution of the X states on the FWM response clearly dominates. The time-resolved FWM signal is emitted as a photon echo that is moderately modulated by the beats between the two polaritons, whereas the time-integrated signal versus the delay between the two laser pulses shows long decay times ($\simeq 10$ ps) and only weak Rabi oscillations. Conversely, the linear response of the microcavity to an external, ultrashort pulse excitation exhibits deep oscillations and subpicosecond exponential decays. The Maxwell-Bloch equations satisfactorily explain our experimental data. In particular, we show that the decay of the time-integrated FWM signal depends strongly on the relative size of the inhomogeneous broadening with respect to the Rabi splitting. For strong inhomogeneous X broadening, the FWM emission is a photon echo, and the decay time of the TI signal is similar to that of bare QW's. In the limit of small inhomogeneous X linewidths (i.e., a Rabi splitting $\geqslant 4$ times the X linewidth), a considerable fraction of the nonlinear polarization does not show any disorder-induced delay, the time-integrated trace versus delay time between the two laser pulses exhibits deep Rabi oscillations, and the decay time approaches that of the (linear) polariton waves. In this limit, the whole X population also experiences important Rabi oscillations, i.e., the microcavity is effectively in the strong-coupling regime.

ACKNOWLEDGMENTS

The authors would like to thank B. Deveaud, S. Haacke, C. Piermarocchi, and V. Savona for helpful discussions. This work was partially supported by the Centro Nazionale delle Ricerche (CNR) and by the *Fonds National Suisse de la Recherche Scientifique* .

[1] C. Weisbuch, M. Nishioka, A. Ishikawa, and Y. Arakawa, Phys. Rev. Lett. **69**, 3314 (1992); R. Houdre, R. P. Stanley, U. Oesterle, M. Ilegems, and C. Weisbuch, *ibid.* **73**, 2043 (1994); Phys. Rev. B **49**, 16 761 (1994); K. Tanaka, T. Nakamura, W. Takamatsu, M. Yamanishi, Y. Lee, and T. Ishira, Phys. Rev. Lett. **74**, 3380 (1995); J. Tignon, P. Voisin, C. Delalande, M. Voos, R. Houdre, U. Oesterle, and R. P. Stanley, *ibid.* **74**, 3967 (1995); A. Tredicucci, Y. Chen, V. Pellegrini, M. Borger, L. Sorba, F. Beltram, and F. Bassani, *ibid.* **75**, 3906 (1995).

[2] V. Savona, Z. Hradil, A. Quattropani, and P. Schwendimann, Phys. Rev. B **49**, 8774 (1994); S. Jorda, Solid State Commun. **93**, 45 (1995); V. Savona, L. C. Andreani, P. Schwendimann, and A. Quattropani, Superlatt. Microstruct. **15**, 433 (1994); I. Abram and J. L. Oudar, Phys. Rev. A **51**, 4116 (1995); F. Tassone, C. Piermarocchi, V. Savona, A. Quattropani, and P. Schwendimann, Phys. Rev. B **53**, 7642 (1996).

[3] Y. Yamamoto, F. M. Matinaga, S. Machida, A. Karlsson, J. Jacobson, G. Bjork, and T. Mukai, J. Phys. (France) IV **3**, 39 (1993).

[4] J. Jacobson, S. Pau, H. Cao, G. Bjork, and Y. Yamamoto, Phys. Rev. A **51**, 2542 (1995).

[5] S. Pau, G. Bjork, J. Jacobson, H. Cao, and Y. Yamamoto, Phys. Rev. B **51**, 14 437 (1995); S. Pau, G. Bjork, J. Jacobson, H. Cao, E. Hanamura, and Y. Yamamoto, Solid State Commun. **98**, 781 (1996).

[6] R. Houdre, R.P. Stanley, and M. Ilegems, Phys. Rev. A **53**, 2711 (1996).

[7] L. C. Andreani and G. Panzarini, Nuovo Cimento **17D**, 1211 (1995); G. Panzarini and L. C. Andreani, Phys. Rev. B **52**, 10 780 (1995).

[8] T. B. Norris, J. K. Rhee, D. S. Citrin, M. Nishioka, and Y. Arakawa, Nuovo Cimento **17D**, 1295 (1995).

[9] H. Wang, J. Shah, T. C. Damen, W. Y. Jan, J. E. Cunningham, M. Hong, and J. P. Mannaerts, Phys. Rev. B **51**, 14 713 (1995).

[10] T. B. Norris, J. K. Rhee, C. Y. Sung, Y. Arakawa, M. Nishioka, and C. Weisbuch, Phys. Rev. B **50**, 14 663 (1994).

[11] M. D. Webb, S. T. Cundiff, and D. G. Steel, Phys. Rev Lett. **66**, 934 (1991); Phys. Rev. B **43**, 12 658 (1991).

[12] R. P. Stanley, R. Houdre, C. Weisbuch, U. Oesterle, and M. Ilegems, Phys. Rev. B **53**, 10 995 (1996).

[13] E. J. Mayer, G. O. Smith, V. Heuckeroth, K. Kuhl, K. Bott, A. Schulze, T. Meier, D. Bennhardt, S. W. Koch, P. Thomas, R.

Hey, and K. Ploog, Phys. Rev. B **50**, 14 730 (1994).
[14] T. Rappen, G. Mohs, and M. Wegener, Phys. Rev. B **47**, 9658 (1993).
[15] D. L. Mills, *Nonlinear Optics* (Springer-Verlag, Berlin, 1991).
[16] T. Yajima and Y. Taira, J. Phys. Soc. Jpn. **47**, 1620 (1979).
[17] The linear susceptibility of a QW is, in principle, not local. The inclusion of nonlocal effects is expected to be necessary to have a better quantitative agreement with the experiments (Ref. 7).
[18] M. Wegener, D. S. Chemla, S. Schmitt-Rink, and W. Schafer, Phys. Rev. B **42**, 5675 (1990).
[19] J. Hegarty and M. D. Sturge, J. Opt. Soc. Am. B **2**, 1143 (1985); S. T. Cundiff, H. Wang, and D. G. Steel, Phys. Rev. B **46**, 7248 (1992).
[20] D. Birkedal, J. Singh, V. G. Lyssenko, J. Erland, and J.M. Hvam, Phys. Rev. Lett **76**, 672 (1996).